J|A|C|S
ARTICLES
Published on Web 03/15/2006

Electron Donor−Bridge−Acceptor Molecules with Bridging Nitronyl Nitroxide Radicals: Influence of a Third Spin on Charge- and Spin-Transfer Dynamics

Erin T. Chernick, Qixi Mi, Richard F. Kelley, Emily A. Weiss, Brooks A. Jones, Tobin J. Marks,* Mark A. Ratner,* and Michael R. Wasielewski*

Contribution from the Department of Chemistry and Center for Nanofabrication and Molecular Self-Assembly, Northwestern University, Evanston, Illinois 60208-3113

Received November 9, 2005; E-mail: m-wasielewski@northwestern.edu

Abstract: Appending a stable radical to the bridge molecule in a donor−bridge−acceptor system (D−B−A) is potentially an important way to control charge- and spin-transfer dynamics through D−B−A. We have attached a nitronyl nitroxide (NN•) stable radical to a D−B−A system having well-defined distances between the components: MeOAn−6ANI−Ph(NN•)−NI, where MeOAn = *p*-methoxyaniline, 6ANI = 4-(*N*-piperidinyl)-naphthalene-1,8-dicarboximide, Ph = phenyl, and NI = naphthalene-1,8:4,5-bis(dicarboximide). MeOAn-6ANI, NN•, and NI are attached to the 1, 3, and 5 positions of the Ph bridge. Using both time-resolved optical and EPR spectroscopy, we show that NN• influences the spin dynamics of the photogenerated triradical states ^{2,4}(MeOAn^{+}•−6ANI−Ph(NN•)−NI^{-}•), resulting in slower charge recombination within the triradical compared to the corresponding biradical lacking NN•. The observed spin−spin exchange interaction between the photogenerated radicals MeOAn^{+}• and NI^{-}• is not altered by the presence of NN•, which only accelerates radical pair intersystem crossing. Charge recombination within the triradical results in the formation of ^{2,4}(MeOAn−6ANI−Ph(NN•)−^{3}*NI), in which NN• is strongly spin-polarized. Normally, the spin dynamics of correlated radical pairs do not produce a net spin polarization; however, net spin polarization appears on NN• with the same time constant as describes the photogenerated radical ion pair decay. This effect is attributed to antiferromagnetic coupling between NN• and the local triplet state ^{3}*NI, which is populated following charge recombination. This requires an effective switch in the spin basis set between the triradical and the three-spin charge recombination product having both NN• and ^{3}*NI present.

Introduction

Electron-transfer reactions are important in applications ranging from solar cells and light-emitting diodes to molecule-based materials for electronics and photonics.[1−16] With regard to the latter, we have developed several approaches to controlling charge transport in organic donor−bridge−acceptor (D−B−A) arrays that take advantage of the speed and efficiency of ultrafast photoinduced electron-transfer reactions.[17−19] However, using spin dynamics to control charge and spin transport properties within molecules is an important aspect of this problem that has received only limited attention. Photogenerated radical pairs are capable of exhibiting coherent spin motion over microsecond time scales,[20,21] which is considerably longer than coherent phenomena involving photogenerated excited states. This affords the possibility that coherent spin motion can provide the basis for novel organic computational devices.[22−32] However, before efficient organic spintronic devices can be realized, a

(1) Wasielewski, M. R. *Chem. Rev.* **1992**, *92*, 435−461.
(2) Gust, D.; Moore, T. A.; Moore, A. L. *Acc. Chem. Res.* **2001**, *34*, 40−48.
(3) Wagner, R. W.; Lindsey, J. S.; Seth, J.; Palaniappan, V.; Bocian, D. F. *J. Am. Chem. Soc.* **1996**, *118*, 3996−3997.
(4) de Silva, A. P.; Gunaratne, H. Q. N.; Gunnlaugsson, T.; Huxley, A. J. M.; McCoy, C. P.; Radmacher, J. T.; Rice, T. E. *Chem. Rev.* **1997**, *97*, 1515−1566.
(5) Willner, I.; Willner, B. *J. Mater. Chem.* **1998**, *8*, 2543−2556.
(6) Tour, J. M.; Kozaki, M.; Seminario, J. M. *J. Am. Chem. Soc.* **1998**, *120*, 8486−8493.
(7) Collier, C. P.; Matterstei, G.; Wong, E. W.; Luo, Y.; Beverly, K.; Sampaio, J.; Raymo, F. M.; Stoddart, J. F.; Heath, J. R. *Science* **2000**, *289*, 1172−1175.
(8) Davis, W. B.; Svec, W. A.; Ratner, M. A.; Wasielewski, M. R. *Nature* **1998**, *396*, 60−63.
(9) Waldeck, D. H.; Beratan, D. N. *Science* **1993**, *261*, 576−577.
(10) Metzger, R. M. *Acc. Chem. Res.* **1999**, *32*, 950−957.
(11) Chen, J.; Reed, M. A.; Rawlett, A. M.; Tour, J. M. *Science* **1999**, *286*, 1550−1552.
(12) Prathapan, S.; Yang, S. I.; Seth, J.; Miller, M. A.; Bocian, D. F.; Holten, D.; Lindsey, J. S. *J. Phys. Chem. B* **2001**, *105*, 8237−8248.
(13) Yang, S. I.; Prathapan, S.; Miller, M. A.; Seth, J.; Bocian, D. F.; Lindsey, J. S.; Holten, D. *J. Phys. Chem. B* **2001**, *105*, 8249−8258.
(14) Ik Yang, S.; Lammi, R. K.; Prathapan, S.; Miller, M. A.; Seth, J.; Diers, J. R.; Bocian, D. F.; Lindsey, J. S.; Holten, D. *J. Mater. Chem.* **2001**, *11*, 2420−2430.
(15) del Rosario Benites, M.; Johnson, T. E.; Weghorn, S.; Yu, L.; Rao, P. D.; Diers, J. R.; Yang, S. I.; Kirmaier, C.; Bocian, D. F.; Holten, D.; Lindsey, J. S. *J. Mater. Chem.* **2002**, *12*, 65−80.
(16) Jones, B. A.; Ahrens, M. J.; Yoon, M.-H.; Facchetti, A.; Marks, T. J.; Wasielewski, M. R. *Angew. Chem., Int. Ed.* **2004**, *43*, 6363−6366.
(17) Gosztola, D.; Niemczyk, M. P.; Wasielewski, M. R. *J. Am. Chem. Soc.* **1998**, *120*, 5118−5119.
(18) Hayes, R. T.; Wasielewski, M. R.; Gosztola, D. *J. Am. Chem. Soc.* **2000**, *122*, 5563−5567.
(19) Lukas, A. S.; Wasielewski, M. R. In *Molecular Switches*; Feringa, B. L., Ed.; Wiley-VCH: Weinheim, 2001; pp 1−35.
(20) Prisner, T.; Dobbert, O.; Dinse, K. P.; van Willigen, H. *J. Am. Chem. Soc.* **1988**, *110*, 1622−1623.
(21) Angerhofer, A.; Toporowicz, M.; Bowman, M. K.; Norris, J. R.; Levanon, H. *J. Phys. Chem.* **1988**, *92*, 7164−7166.
(22) Rajca, A. *Chem. Rev.* **1994**, *94*, 871−893.
(23) Nakatsuji, S.; Anzai, H. *J. Mater. Chem.* **1997**, *7*, 2161−2174.
(24) Lahti, P. M., Ed. *Magnetic Properties of Organic Materials*; Marcel Dekker: New York, 1999.

10.1021/ja0576435 CCC: $33.50

greater fundamental understanding of the factors controlling spin dynamics in complex organic donor−acceptor systems must be obtained.

The presence of additional unpaired spins provided by stable free radicals and triplet-state molecules (e.g. oxygen) has been shown to increase the rate of radical pair intersystem crossing (RP-ISC) between photogenerated singlet and triplet radical pairs.[32−36] For molecules in which the stable radical and the photoactive system are connected by a flexible covalent linkage, the resulting large degree of conformational freedom translates into a distribution of distances and spin−spin interaction strengths that complicate the analysis of the spin dynamics.[37−40] Our approach to studying the influence of spin dynamics on charge and spin transport in D−B−A molecules strongly restricts conformational freedom and controls electronic coupling between each component of a D−B−A molecule having a stable radical covalently bound to it. For example, we recently demonstrated[41] that covalently attaching a 2,2,6,6-tetramethyl-1-piperidinyloxyl (TEMPO) stable free radical to the acceptor terminus of a rigid D−B−A molecule perturbs charge recombination rates via an enhanced intersystem crossing (EISC) mechanism similar to that observed for intermolecular systems,[32,33,35] while not altering the spin−spin exchange interaction within the photogenerated radical ion pair.

These results, along with the fact that the structural and electronic properties of the bridge molecule within a D−B−A system are critical to determining the rate of electron (or hole) transfer from D to A,[42] prompted us to explore how a stable paramagnetic center (a radical or radical ion) attached directly to the bridge molecule of a D−B−A system affects the dynamics of photoinduced charge and spin transport. Nitronyl nitroxide (NN•) is a stable, easily functionalized radical that has been studied extensively in the organic magnetic materials field.[43−49] The spin density distribution of NN• is localized largely on its two N−O groups and not on the molecule to which NN• is appended,[50] so that attachment of NN• to B within D−B−A does not result in significant spin delocalization onto B itself. Modulating the degree of spin delocalization from the appended radical onto B is potentially an important means to control the electron-transfer dynamics through B, and the work presented here is the first step toward this goal. We have chosen to modify a previously well-characterized D−B−A system to test these ideas, MeOAn−6ANI−Ph−NI (**8**),[51,52] where MeOAn = *p*-methoxyaniline, 6ANI = 4-(*N*-piperidinyl)naphthalene-1,8-dicarboximide, Ph = phenyl, and NI = naphthalene-1,8:4,5-bis(dicarboximide).[51] We have now synthesized an analogue to this system, MeOAn−6ANI−Ph(NN•)−NI (**7**), in which MeOAn−6ANI, NN•, and NI are attached to the 1, 3, and 5 positions, respectively, of the Ph bridge. Here we report on the influence of NN• on both electron transfer and spin dynamics in **7**, studied using time-resolved optical and EPR spectroscopy.

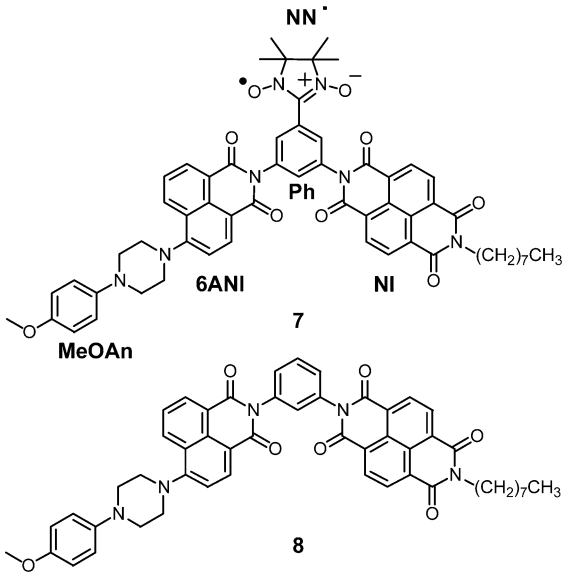

Experimental Section

The synthesis and characterization of compound **7** are described in the Supporting Information. Compound **7** was purified by preparative TLC on alumina. All solvents were spectrophotometric grade or distilled prior to use.

Ground-state absorption measurements were made on a Shimadzu (UV-1601) spectrophotometer. The optical density of all samples was maintained between 0.3 and 0.6 at 420 nm ($\epsilon_{6ANI,420\ nm} = 7000\ cm^{-1}\ M^{-1}$) for both femtosecond and nanosecond transient absorption spectroscopy. Femtosecond transient absorption measurements were made using the 420 nm frequency-doubled output from a regeneratively amplified titanium−sapphire laser system operating at 2 kHz as the

(25) Crayston, J. A.; Devine, J. N.; Walton, J. C. *Tetrahedron* **2000**, *56*, 7829−7857.
(26) Sugawara, T., Sakurai, H., Izuoka, A., Eds. *Electronically controllable high spin systems realized by spin-polarized donors*; Gordon and Breach: Amsterdam, 2001.
(27) Wolf, S. A.; Awschalom, D. D.; Buhrman, R. A.; Daughton, J. M.; von Molnar, S.; Roukes, M. L.; Chtchelkanova, A. Y.; Treger, D. M. *Science* **2001**, *294*, 1488−1495.
(28) Miller, J. S.; Manson, J. L. *Acc. Chem. Res.* **2001**, *34*, 563−570.
(29) Awschalom, D. D.; Flatte, M. E.; Samarth, N. *Sci. Am.* **2002**, *286*, 67−73.
(30) Rajca, A. *Chem. Eur. J.* **2002**, *8*, 4834−4841.
(31) Itkis, M. E.; Chi, X.; Cordes, A. W.; Haddon, R. C. *Science* **2002**, *296*, 1443−1445.
(32) Buchachenko, A. L.; Berdinsky, V. L. *Chem. Rev.* **2002**, *102*, 603−612.
(33) Buchachenko, A. L.; Ruban, L. V.; Step, E. N.; Turro, N. J. *Chem. Phys. Lett.* **1995**, *233*, 315−318.
(34) Vlassiouk, I.; Smirnov, S.; Kutzki, O.; Wedel, M.; Montforts, F.-P. *J. Phys. Chem. B* **2002**, *1−6*, 8657−8666.
(35) Smirnov, S.; Vlassiouk, I.; Kutzki, O.; Wedel, M.; Montforts, F.-P. *J. Am. Chem. Soc.* **2002**, *124*, 4212−4213.
(36) Volkova, O. S.; Taraban, M. B.; Plyusnin, V. F.; Leshina, T. V.; Egorov, M. P.; Nefedov, O. M. *J. Phys. Chem. A* **2003**, *107*, 4001−4005.
(37) Mori, Y.; Sakaguchi, Y.; Hayashi, H. *J. Phys. Chem. A* **2002**, *106*, 4453−4467.
(38) Mori, Y.; Sakaguchi, Y.; Hayashi, H. *Bull. Chem. Soc. Jpn.* **2001**, *74*, 293−304.
(39) Ishii, K.; Hirose, Y.; Kobayashi, N. *J. Phys. Chem. A* **1999**, *103*, 1986−1990.
(40) Ishii, K.; Hirose, Y.; Fujitsuka, H.; Ito, O.; Kobayashi, N. *J. Am. Chem. Soc.* **2001**, *123*, 702−708.
(41) Weiss, E. A.; Chernick, E. T.; Wasielewski, M. R. *J. Am. Chem. Soc.* **2004**, *126*, 2326−2327.
(42) Weiss, E. A.; Wasielewski, M. R.; Ratner, M. A. *Top. Curr. Chem.* **2005**, *257*, 103−133.
(43) Moigne, J. L.; Gallani, J. L.; Wautelet, P.; Moroni, M.; Oswald, L.; Cruz, C.; Galerne, Y.; Arnault, J. C.; Duran, R.; Garrett, M. *Langmuir* **1998**, *14*, 7484−7492.
(44) Zhang, D.; Xu, Y.; Ding, L.; Liu, Y.; Zhu, D. *Chem. Phys. Lett.* **1999**, *304*, 236−240.
(45) Matsuura, H.; Tamura, R.; Yamauchi, J. *Synth. Met.* **2003**, *133−134*, 605−607.
(46) Yamaguchi, K.; Namimoto, H.; Fueno, T.; Nogami, T.; Shirota, Y. *Chem. Phys. Lett.* **1990**, *166*, 408−414.
(47) Yamaguchi, K.; Okumura, M.; Fueno, T.; Nakasuji, K. *Synth. Met.* **1991**, *43*, 3631−3634.
(48) Hiraoka, S.; Okamoto, T.; Kozaki, M.; Shiomi, D.; Sato, K.; Takui, T.; Okada, K. *J. Am. Chem. Soc.* **2004**, *126*, 58−59.
(49) Nagashima, H.; Inoue, H.; Yoshioka, N. *J. Phys. Chem. B* **2004**, *108*, 6144−6151.
(50) Davis, M. S.; Kreilick, R. W.; Morokuma, K. *J. Am. Chem. Soc.* **1972**, *94*, 5588−5592.
(51) Lukas, A. S.; Bushard, P. J.; Weiss, E. A.; Wasielewski, M. R. *J. Am. Chem. Soc.* **2003**, *125*, 3921−3930.
(52) Shaakov, S.; Galili, T.; Stavitski, E.; Levanon, H.; Lukas, A.; Wasielewski, M. R. *J. Am. Chem. Soc.* **2003**, *125*, 6563−6572.

excitation pulse and a white light continuum probe pulse as described earlier.[53] Samples were placed in a 2 mm path length glass cuvette and stirred using a motorized wire stirrer to prevent thermal lensing and sample degradation. The samples were irradiated with 0.5−1.0 μJ/pulse focused to a 200 μm spot. The total instrument response time for the pump−probe experiments was 150 fs. Transient absorption kinetics were fit to a sum of exponentials with a Gaussian instrument function using Levenberg−Marquardt least-squares fitting.

Samples for nanosecond transient absorption spectroscopy were placed in a 10 mm path length quartz cuvette equipped with a vacuum adapter and subjected to five freeze−pump−thaw degassing cycles. The samples were excited with 5 ns, 1 mJ, 420 nm laser pulses generated using the frequency-tripled output of a Continuum 8000 Nd:YAG laser to pump a Continuum Panther OPO. The excitation pulse was focused to a 5 mm diameter spot and matched to the diameter of the probe pulse generated using a xenon flashlamp (EG&G Electro-Optics FX-200). The signal was detected using a photomultiplier tube with high voltage applied to only four dynodes (Hamamatsu R928). The total instrument response time is 7 ns and is determined primarily by the laser pulse duration. The sample cuvette was placed between the poles of a Walker Scientific HV-4W electromagnet powered by a Walker Magnion HS-735 power supply. The field strength was measured by a Lakeshore 450 gaussmeter with a Hall effect probe. Both the electromagnet and the gaussmeter were interfaced with the data collection computer, allowing measurement and control of the magnetic field to $\pm 1 \times 10^{-5}$ T during data acquisition. Due to the length of the sample runs (>3 h), a small amount of sample degradation was observed, resulting in a decrease in the triplet yield at zero field, $\Delta A(B = 0)$, over the course of the experiments. To compensate for this, the magnetic field was reset to $B = 0$ mT every three kinetic traces and $\Delta A(B = 0)$ was plotted and fit with a polynomial or series of polynomials. These functions were used to calculate the relative triplet yield or RP yield as a function of applied field strength. The relative triplet yield is thus:

$$\frac{T}{T_0} = \frac{\Delta A(B)}{\Delta A(B = 0)}$$

The results presented are averages of three or more experiments conducted on separate days with freshly prepared samples in spectrophotometric or freshly distilled ACS grade toluene.

For EPR measurements, a toluene solution of **7** (0.2 mM) was loaded into a quartz tube (4 mm o.d. × 2 mm i.d.) and subjected to five freeze−pump−thaw degassing cycles on a vacuum line (10^{-4} mbar). The tube was then sealed using a hydrogen torch and kept in the dark when not being used. The sample was excited using 416 nm, 1 mJ, 7 ns laser pulses from the H_2-Raman shifted output of a frequency-tripled, Q-switched Nd:YAG laser (Quanta Ray DCR-2).

Steady-state EPR spectra, transient CW EPR spectra, and pulse EPR spectra were measured using a Bruker Elexsys E580 X-band EPR spectrometer with a variable-Q dielectric resonator (Bruker ER 4118X-MS5) at room temperature. Steady-state CW EPR spectra were measured under the conditions of 0.2−2 mW microwave power and 0.01−0.05 mT field modulation at 100 kHz. The g values of the spectra were calibrated with a crystalline 2,2-diphenyl-1-picrylhydrazyl (DPPH) standard ($g = 2.0036$). Transient CW EPR measurements were carried out under CW microwave irradiation (typically 2−20 mW) by accumulating kinetic traces of transient magnetization following photoexcitation. The field modulation was disabled to achieve a response time $\tau = Q/\pi\nu \approx 30$ ns,[54] and microwave signals in emission (e) and/or absorption (a) were detected in both the real and the imaginary channels (quadrature detection). Sweeping the magnetic field gave 2D complex spectra versus time and magnetic field. For each kinetic trace, the signal acquired prior to the laser pulse was subtracted from the data. Kinetic traces recorded off-resonance were considered background signals, whose average was subtracted from all kinetic traces. The spectra were subsequently phased into a Lorentzian part and a dispersive part, and the former, also known as the imaginary magnetic susceptibility χ'', is presented.

High-power microwave pulses were generated by a 1-kW TWT amplifier (Applied Systems Engineering 117X). The typical length of a $\pi/2$ pulse was 8 ns. The resonator was fully overcoupled to achieve $Q < 200$ and a dead time of ~72 ns. All the quadrature-detected spectra were properly phased, and χ'' is presented. In the pulse EPR kinetic measurements, the first microwave pulse was initially applied 200 ns before the laser pulse and then was delayed incrementally relative to the laser pulse. A kinetic trace was formed by measuring the intensity of the free induction decay (FID) at different time delays of the microwave pulse with respect to the laser pulse.

Results

Synthesis. The synthesis of **8** has been reported previously,[51] and the complete synthesis of radical **7** is outlined in Scheme 1. Commercially available 3,5-dinitrobenzyl alcohol was protected with a triisopropylsilyl (TIPS) group, followed by reduction of the nitro groups to yield **2** (71%). Imide coupling of the known MeOAn-6ANI anhydride[41] with diamine **2** yields **3** (80%). Due to the decrease in nucleophilicity of the remaining amino group in **3** following the first imide coupling, the subsequent imide coupling of the NI acceptor proved to be inefficient, giving **4** in a modest 59% yield. Deprotection of the TIPS group was accomplished with TBAF at −20 °C in THF, giving alcohol **5** in 97% yield. We observed that deprotection does not occur at −78 °C, while the NI group is cleaved if the reaction is allowed to occur at room temperature. Subsequent oxidation of the alcohol to the corresponding aldehyde with fresh barium manganate yields **6** in quantitative yield. Formation of the nitronyl nitroxide was accomplished using slight modifications to Ullman's procedure.[55−58] 2,3-Bis-(hydroxamino)-2,3-dimethylbutane sulfate was condensed with aldehyde **6** in dimethyl sulfoxide to form the tetramethylimidazolidine intermediate. Attempts to use the typical methanol/water solvent system for this reaction failed due to the insolubility of the aldehyde precursor. The oxidation of the tetramethylimidazolidine intermediate was accomplished with sodium periodate in a biphasic system of water and methylene chloride to give **7** in 22% yield.

Steady-State Properties. The photophysical properties of 6ANI, NI, and **8** have been characterized previously in detail.[51,52,59,60] In summary, the ground-state optical spectrum of 6ANI exhibits a broad charge-transfer (CT) band centered at 390 nm, while that of NI exhibits three distinct absorptions due to vibronic structure on the $\pi-\pi^*$ transition at 343, 363, and 382 nm. In MeOAn−6ANI−Ph(NN•)−NI there is an additional predominant absorption belonging to NN• at 368 nm, which overlaps the absorptions of both 6ANI and NI (Figure

(53) Giaimo, J. M.; Gusev, A. V.; Wasielewski, M. R. *J. Am. Chem. Soc.* **2002**, *124*, 8530−8531.
(54) Schweiger, A.; Jeschke, G. *Principles of pulse electron paramagnetic resonance*; Oxford University Press: Oxford, 2001.
(55) Ullman, E. F.; Osiecki, J. H.; Boocock, D. G. B.; Darcy, R. *J. Am. Chem. Soc.* **1972**, *94*, 7049−7059.
(56) Hirel, C.; Vostrikova, K. E.; Pecaut, J.; Ovcharenko, V. I.; Rey, P. *Chem. Eur. J.* **2001**, *7*, 2007−2014.
(57) Osiecki, J. H.; Ullman, E. F. *J. Am. Chem. Soc.* **1968**, *90*, 1078−1079.
(58) Klyatskaya, S. V.; Tretyakov, E. V.; Vasilevsky, S. F. *Russ. Chem. Bull., Int. Ed.* **2002**, *51*, 128−134.
(59) Greenfield, S. R.; Svec, W. A.; Gosztola, D.; Wasielewski, M. R. *J. Am. Chem. Soc.* **1996**, *118*, 6767−6777.
(60) Debreczeny, M. P.; Svec, W. A.; Marsh, E. M.; Wasielewski, M. R. *J. Am. Chem. Soc.* **1996**, *118*, 8174−8175.

Scheme 1 [a]

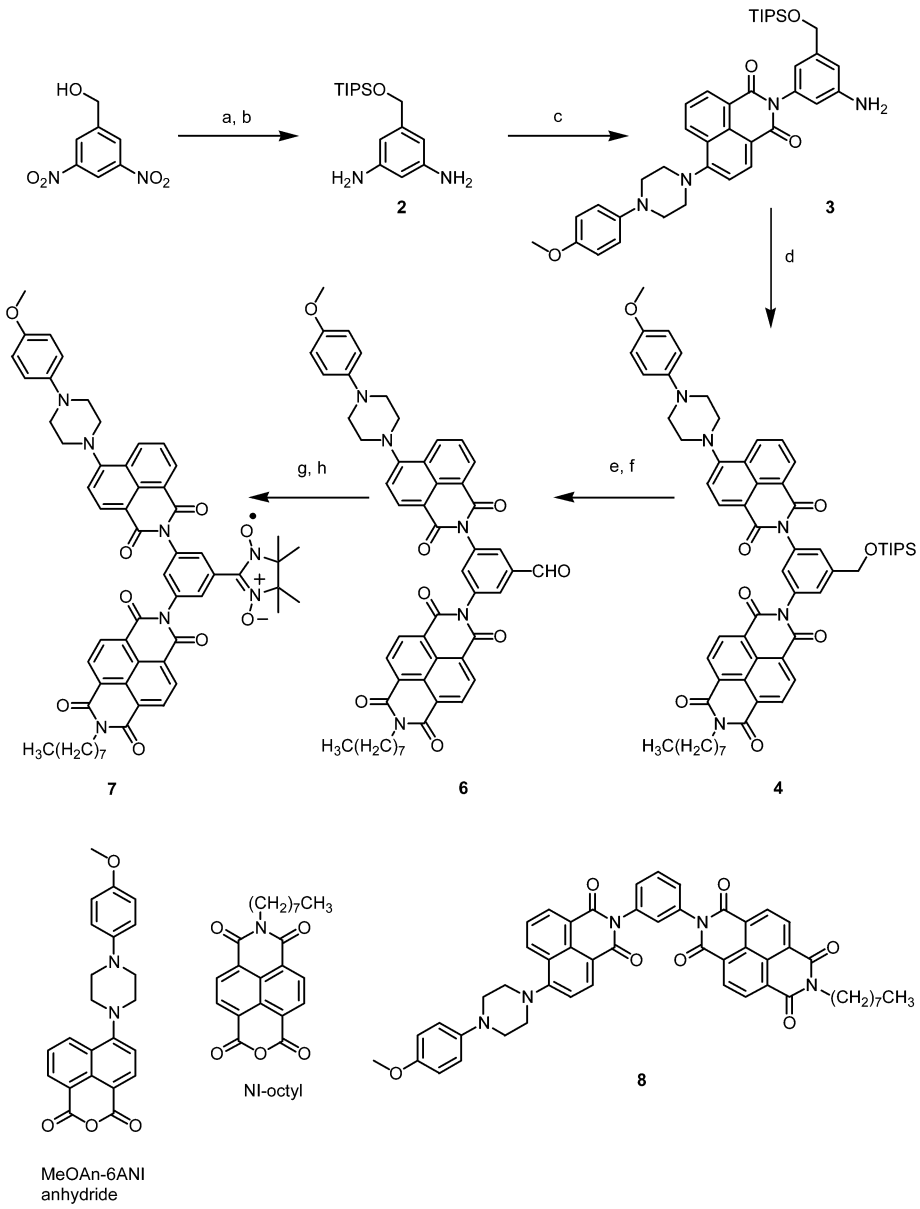

[a] Reagents and conditions: (a) TIPSCl, imidazole, DMF, reflux, 71%; (b) Pd/C, H_2, 32 psi, quantitative; (c) MeOAn-6ANI anhydride, pyridine, imidazole, reflux, 80%; (d) NI−octyl anhydride, pyridine, imidazole, reflux, 59%; (e) TBAF, THF, −20 °C, 97%; (f) $BaMnO_4$, CH_2Cl_2, quantitative; (g) 2,3-bis(hydroxamino)-2,3-dimethylbutane sulfate, DMSO; (h) $NaIO_4$, H_2O, CH_2Cl_2, 22%.

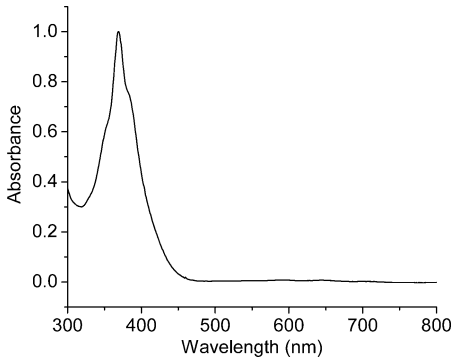

Figure 1. UV−vis spectrum of **7** in toluene.

1). There is also a weak, broad absorption due to NN• near 600 nm. The redox potentials of MeOAn−6ANI−Ph−NI have been described in detail elsewhere.[51,59] Briefly, the first oxidation potential of ANI occurs at 1.22 V and the first reduction potential of NI is −0.53 V. These redox potentials are assumed not to differ significantly in MeOAn−6ANI−Ph(NN•)−NI. The one-electron potentials for oxidation and reduction of NN• are approximately 0.82 and −1.25 V vs SCE, respectively.[61,62]

The energy levels of the excited and charge-separated species for **8** have been calculated previously using the Weller equation.[51] It is assumed that there is no significant change in these levels when the nitronyl nitroxide free radical is appended to the bridge, so that the energy level diagram displayed in Figure 2 is representative of both radical **7** and model compound **8**.

Time-Resolved Charge Separation and Recombination Dynamics. Femtosecond transient absorption spectroscopy allows for the direct observation of the intermediates involved

(61) Sakurai, H.; Izuoka, A.; Sugawara, T. *J. Am. Chem. Soc.* **2000**, *122*, 9723−9734.
(62) Ziessel, R.; Ulrich, G.; Lawson, R. C.; Echegoyen, L. *J. Mater. Chem.* **1999**, *9*, 1435−1448.

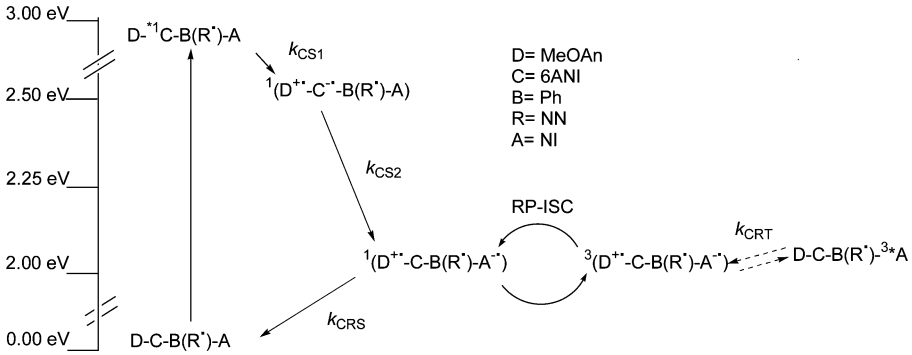

Figure 2. Energy level diagram for compound **7**.

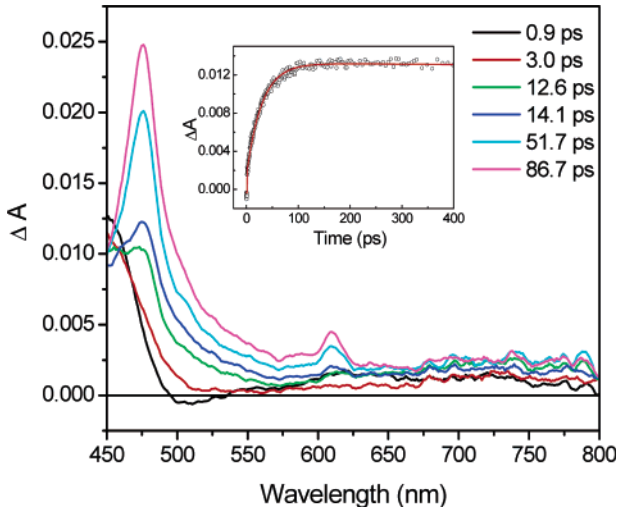

Figure 3. Femtosecond transient absorption spectra of **7** in toluene obtained at the indicated times following a 420 nm, 100 fs laser pulse. Inset: A kinetic trace obtained at 495 nm.

in charge separation (CS) (Figure 3). Photoexcitation of 6ANI with a 420 nm, 100 fs laser pulse results in the reaction MeOAn−^{1}*6ANI−Ph(NN•)−NI → MeOAn^{+}•−6ANI^{-}•−Ph(NN•)−NI with a time constant $\tau_{CS1} = 11$ ps, as indicated by the formation of an absorption band (shoulder) due to MeOAn^{+}• near 510 nm. Subsequently, the absorption features characteristic of NI^{-}• at 480 and 610 nm appear with $\tau_{CS2} = 31$ ps, indicating that the reaction MeOAn^{+}•−6ANI^{-}•−Ph(NN•)−NI → MeOAn^{+}•−6ANI−Ph(NN•)−NI^{-}• has occurred. The transient spectra are similar to those observed earlier for **8**,[51] and hence, there is no evidence from the transient absorption data that NN• is either oxidized or reduced in this process. The time constants for this sequential charge separation process are comparable to those reported earlier for MeOAn−6ANI−Ph−NI, where $\tau_{CS1} = 8$ ps and $\tau_{CS2} = 40$ ps.

The magnetic field effect (MFE) on the rate and yield of radical ion pair (RP) recombination directly reveals the magnitude of electron spin−spin exchange interaction, 2*J*, between the spins within the RP, which is proportional to the square of the donor−acceptor superexchange coupling, V_{DA}.[63−66] The mechanistic details of the RP-ISC mechanism and the theory behind the MFE have been researched extensively[67−70] and applied to many donor−acceptor systems,[51,63,71−77] including biological[68,78−81] systems. For example, photoexcitation of model compound **8**, which lacks NN•, initially produces the singlet RP, which undergoes electron−nuclear hyperfine coupling-induced RP-ISC to produce the triplet RP, ^{1}(MeOAn^{+}•−6ANI−Ph−NI^{-}•) → ^{3}(MeOAn^{+}•−6ANI−Ph−NI^{-}•). The subsequent charge recombination process is spin selective; i.e., the singlet RP recombines to the singlet ground state and the triplet RP recombines to yield the neutral local triplet MeOAn−6ANI−Ph−^{3}*NI. Application of a static magnetic field splits the RP triplet levels, and variation of the field strength modulates the efficiency of the ISC by adjusting the energies of triplet sublevels relative to that of the singlet level. When the Zeeman splitting of the triplet RP levels equals the intrinsic singlet−triplet splitting, 2*J*, of the RP, there is an increase in intersystem crossing rate. This increase translates into a maximum in triplet RP production and therefore a maximum in local triplet production upon recombination. By monitoring the yield of local triplet production as a function of applied magnetic field, the magnitude of the magnetic superexchange interaction, *2J*, can be measured directly.[82,83]

The same two rapid, nonadiabatic charge separation steps occur in radical **7**, even though the initial state is formally a doublet, as will be discussed in detail below. Figure 4 shows the MFE on the yield of MeOAn−6ANI−Ph(NN•)−^{3}*NI resulting from charge recombination. The data for **7** show a

(63) Weiss, E. A.; Ahrens, M. J.; Sinks, L. E.; Gusev, A. V.; Ratner, M. A.; Wasielewski, M. R. *J. Am. Chem. Soc.* **2004**, *126*, 5577−5584.
(64) Kobori, Y.; Sekiguchi, S.; Akiyama, K.; Tero-Kubota, S. *J. Phys. Chem. A* **1999**, *103*, 5416−5424.
(65) Paddon-Row, M. N.; Shephard, M. J. *J. Phys. Chem. A* **2002**, *106*, 2935−2944.
(66) Volk, M.; Haberle, T.; Feick, R.; Ogrodnik, A.; Michel-Beyerle, M. E. *J. Phys. Chem.* **1993**, *97*, 9831−9836.
(67) Weller, A.; Staerk, H.; Treichel, R. *Faraday Discuss., Chem. Soc.* **1984**, *78*, 271−278.
(68) Hoff, A. J.; Gast, P.; van der Vos, R.; Franken, E. M.; Lous, E. J. *Z. Phys. Chem.* **1993**, *180*, 175−192.
(69) Till, U.; Hore, P. J. *Mol. Phys.* **1997**, *90*, 289−296.
(70) Steiner, U. E.; Ulrich, T. *Chem. Rev.* **1989**, *89*, 51−147.
(71) Schulten, K.; Staerk, H.; Weller, A.; Werner, H.-J.; Nickel, B. *Z. Phys. Chem.* **1976**, *101*, 371−390.
(72) Tanimoto, Y.; Okada, N.; Itoh, M.; Iwai, K.; Sugioka, K.; Takemura, F.; Nakagaki, R.; Nagakura, S. *Chem. Phys. Lett.* **1987**, *136*, 42−46.
(73) Sakaguchi, Y.; Hayashi, H. *J. Phys. Chem. A* **1997**, *101*, 549−555.
(74) Werner, U.; Kuhnle, W.; Staerk, H. *J. Phys. Chem.* **1993**, *97*, 9280−9287.
(75) Weiss, E. A.; Ratner, M. A.; Wasielewski, M. R. *J. Phys. Chem. A* **2003**, *107*, 3639−3647.
(76) Tadjikov, B.; Smirnov, S. *Phys. Chem. Chem. Phys.* **2001**, *3*, 204−212.
(77) Tsentalovich, Y. P.; Morozova, O. B.; Avdievich, N. I.; Ananchenko, G. S.; Yurkovskaya, A. V.; Ball, J. D.; Forbes, M. D. E. *J. Phys. Chem. A* **1997**, *101*, 8809−8816.
(78) Blankenship, R. E.; Schaafsma, T. J.; Parson, W. W. *Biochim. Biophys. Acta* **1977**, *461*, 297−305.
(79) Plato, M.; Möbius, K.; Michel-Beyerle, M. E.; Bixon, M.; Jortner, J. *J. Am. Chem. Soc.* **1988**, *110*, 7279−7285.
(80) Werner, H.-J.; Schulten, K.; Weller, A. *Biochim. Biophys. Acta* **1978**, *502*, 255−268.
(81) Norris, J. R.; Bowman, M. K.; Budil, D. E.; Tang, J.; Wraight, C. A.; Closs, G. L. *Proc. Natl. Acad. Sci. U.S.A.* **1982**, *79*, 5532−5536.
(82) Anderson, P. W. *Phys. Rev.* **1959**, *115*, 2−13.
(83) Shultz, D. A.; Fico, R. M., Jr.; Bodnar, S. H.; Kumar, R. K.; Vostrikova, K. E.; Kampf, J. W.; Boyle, P. D. *J. Am. Chem. Soc.* **2003**, *125*, 11761−11771.

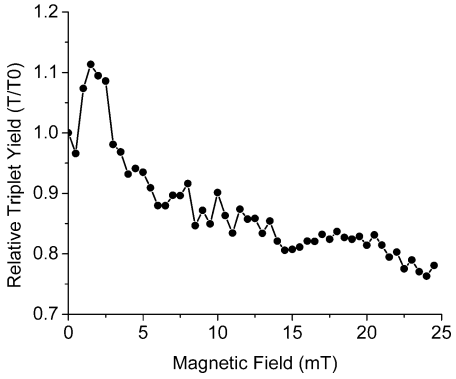

Figure 4. Relative triplet yield of **7** in toluene as a function of magnetic field strength.

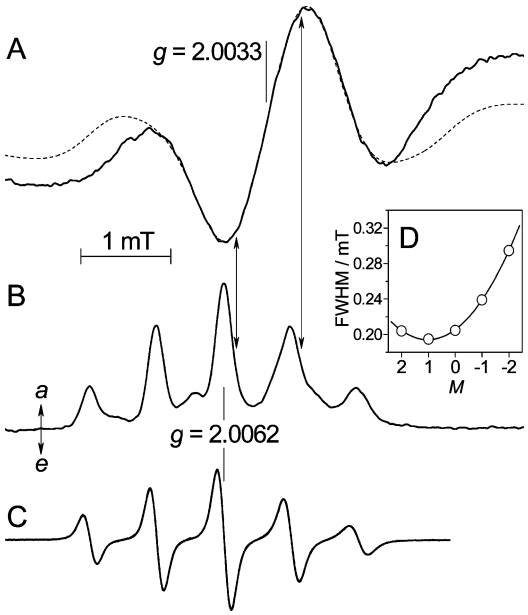

Figure 5. Continuous wave (CW) EPR spectra of **7** in toluene at room temperature, measured (A) 60 and (B) 320 ns after laser excitation, and (C) in steady state in the dark. Note that spectrum C is given in the derivative form. (D) Hyperfine dependence of the line widths (full width at half-maximum, fwhm) of the individual peaks in spectrum C. Dashed line in spectrum A is the numerical simulation to reveal $\Delta_{DQ} = 1.3$ mT.

clear resonance at 1.5 ± 0.3 mT, which is very similar to that observed for model system **8**. The data indicate that the presence of NN• on the Ph bridge does not perturb the magnitude of the spin−spin exchange interaction between the MeOAn$^{+\bullet}$ and NI$^{-\bullet}$ radicals.

EPR Spectroscopy. The steady-state EPR spectrum of **7** consists of five hyperfine lines centered at $g = 2.0062$ due to the two equivalent nitrogens of NN• having $|a_N| = 0.745$ mT (Figure 5C), which is similar to that reported earlier for nitronyl nitroxides.[55] In contrast to unsubstituted nitronyl nitroxides, the line widths of the hyperfine peaks of **7** are quadratically dependent on the overall nuclear quantum number M (Figure 5D), signifying relatively slow rotational averaging of the g and hyperfine anisotropies[84] in the large D−B−A system.

At room temperature in toluene, molecular tumbling renders the EPR spectra of triplet states broad and structureless,[85] if

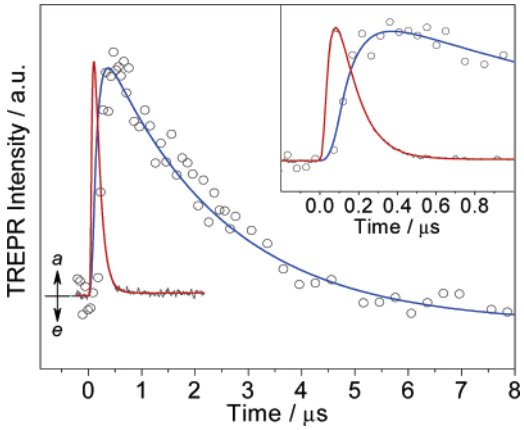

Figure 6. Time-resolved EPR kinetics of the RP state (red) and transiently polarized NN• (blue) of **7** after laser excitation ($t = 0$), measured in toluene at room temperature. The red curve is the difference between two transient CW kinetic traces obtained at field values of 339.3 and 340.0 mT, as indicated by the double-arrow lines in Figure 5, to cancel out the uniform *a* signal from the polarized NN•, whereas the blue curve is measured by the FID intensities of the polarized NN• at various times after laser excitation (see text). Inset: The decay of the RP state matches the rise of polarization at NN•.

not completely undetectable. Thus, time-resolved EPR (TREPR) spectra (i.e., pulsed laser excitation, CW microwaves) were measured around $g \approx 2$, the region where RPs and stable radicals are observed. Immediately after laser excitation, an intense photogenerated RP signal with an *emission*, *absorption* (*e a*) polarization pattern appears (Figure 5A), centered at $g = 2.0033$, similar to the g values of MeOAn$^{\bullet+}$ and NI$^{\bullet-}$.[52] As the RP decays, a new set of peaks with enhanced absorption grow in (Figure 5B) which have g factors, hyperfine splittings, and line widths identical to those measured for NN• in the steady state. Thus, NN• is transiently polarized following charge recombination of the RP state.

To obtain a kinetic trace of the RP state alone, the raw data traces from the TREPR spectra at 340.0 and 339.3 mT were subtracted, so that the uniform *a* signal from the polarized NN• cancels out, while the *e a* signal from the RP state gets doubled (Figure 6). Furthermore, the kinetic behavior of the transient polarization at NN• was monitored using the magnitude of its FID with pulse EPR, a technique with better temporal fidelity at long times than transient CW methods.[86] Moreover, in contrast to doublet-state radicals, the FID from a spin-correlated RP is suppressed by a $\pi/2$ microwave pulse,[87−89] and thus does not interfere with selective observation of the polarized NN• radical. The two kinetic traces in Figure 6 are both well fit with a rise−decay biexponential model, yielding the charge recombination lifetime of the RP state, $\tau_{CR} = 101$ ns, and the rise and decay time of the NN• polarization $\tau_1 = 95 \pm 7$ ns and $\tau_2 = 2.3 \pm 0.2$ μs, respectively. Notably, the decay of the RP state matches the rise of polarization at NN•, the implications of which will be discussed later in this paper, and the decay lifetime of the

(84) Carrington, A.; McLachlan, A. D. *Introduction to magnetic resonance with applications to chemistry and chemical physics*; Harper & Row: New York, 1967.
(85) Yamauchi, S. *Bull. Chem. Soc. Jpn.* **2004**, *77*, 1255−1268.
(86) McLauchlan, K. A. In *Modern pulsed and continuous-wave electron spin resonance*; Kevan, L., Bowman, M. K., Eds.; Wiley: New York, 1990; pp 285−363.
(87) Hasharoni, K.; Levanon, H.; Tang, J.; Bowman, M. K.; Norris, J. R.; Gust, D.; Moore, T. A.; Moore, A. L. *J. Am. Chem. Soc.* **1990**, *112*, 6477−6481.
(88) Timmel, C. R.; Hore, P. J. *Chem. Phys. Lett.* **1994**, *226*, 144−150.
(89) Weis, V.; van Willigen, H. *J. Porphyrins Phthalocyanines* **1998**, *2*, 353−361.

NN• polarization conforms to the spin−lattice relaxation time T_1 of nitroxides at room temperature.[90]

Discussion

Intersystem Crossing. The lifetime of MeOAn$^{+\bullet}$−6ANI−Ph(NN•)−NI$^{-\bullet}$ (τ_{CR} = 101 ns) is significantly longer than that of MeOAn$^{+\bullet}$−6ANI−Ph−NI$^{-\bullet}$ (τ_{CR} = 73 ns).[51] In both cases, charge recombination (CR) leading to the ground state lies deep within the Marcus inverted region[91] because $-\Delta G_{CR} \gg \lambda$, where λ = 0.54 eV,[92] and the rate of this process is therefore expected to be relatively slow. The slower charge recombination in MeOAn$^{+\bullet}$−6ANI−Ph(NN•)−NI$^{-\bullet}$ compared to MeOAn$^{+\bullet}$−6ANI−Ph−NI$^{-\bullet}$ is attributed to EISC induced by the magnetic field of NN•, which increases the rate of mixing between ^{2}(MeOAn$^{+\bullet}$−6ANI−Ph(NN•)−NI$^{-\bullet}$) and ^{2,4}(MeOAn$^{+\bullet}$−6ANI−Ph(NN•)−NI$^{-\bullet}$).[32,34,39,93] Similar effects have been reported in D−B−A molecules having a TEMPO radical attached.[34,38,93−95] The energy level diagram for radical **7** (Figure 2) shows that, for the CR reaction, ^{2,4}(MeOAn$^{+\bullet}$−6ANI−Ph(NN•)−NI$^{-\bullet}$) is nearly isoenergetic with ^{2,4}(MeOAn−6ANI−Ph(NN•)−^{3}*NI), so that an equilibrium between these two species is established.[52,96] EISC shifts the time-integrated population from ^{2}(MeOAn$^{+\bullet}$−6ANI−Ph(NN•)−NI$^{-\bullet}$) to ^{2,4}(MeOAn$^{+\bullet}$−6ANI−Ph(NN•)−NI$^{-\bullet}$) in **7**, which creates a bottleneck to overall charge recombination due to the fact that formation of ^{2,4}(MeOAn−6ANI−Ph(NN•)−^{3}*NI) does not provide a fast exit channel for the charge-separated state. Therefore, the overall rate of charge recombination is slowed, similar to what we observed previously for a MeOAn−6ANI−NI derivative in which a TEMPO radical was rigidly bound to the terminus of the NI acceptor group.[41] This effect is analyzed in terms of the spin dynamics of the system in more detail below.

Electron Spin−Spin Couplings in the Photogenerated Triradical. Following photoexcitation of **7**, the triradical MeOAn$^{\bullet+}$−6ANI−Ph(NN•)−NI$^{\bullet-}$ has three pairs of exchange interactions, $2J_{12}$, $2J_{13}$, and $2J_{23}$, where the subscripts 1, 2, and 3 denote the spins on MeOAn$^{\bullet+}$, NI$^{\bullet-}$, and NN•, respectively. Mori et al.[37] studied a NI$^{\bullet-}$−TEMPO• biradical anion with a spin−spin distance of 8.44 Å and four σ bonds between the two radicals and estimated the exchange coupling $2J$ to be ~1 T (10^{-4} eV). The exchange interaction $2J_{23}$ between the two paramagnetic centers NN• and NI$^{\bullet-}$ in **7** is assumed to be similar because these radicals are also 8.5 Å apart (center-to-center, MM+, Hyperchem[97]) and have four intervening σ bonds. The magnitude of this interaction is similar to that estimated previously by our group for a MeOAn−6ANI−NI derivative in which a TEMPO radical was rigidly bound to the terminus of the NI acceptor group at a similar overall distance.[41] Molecular modeling of **7** shows that the π systems of 6ANI and NI are nearly perpendicular to that of the Ph bridge, so enhanced spin−spin coupling via the π electrons is unlikely.[51]

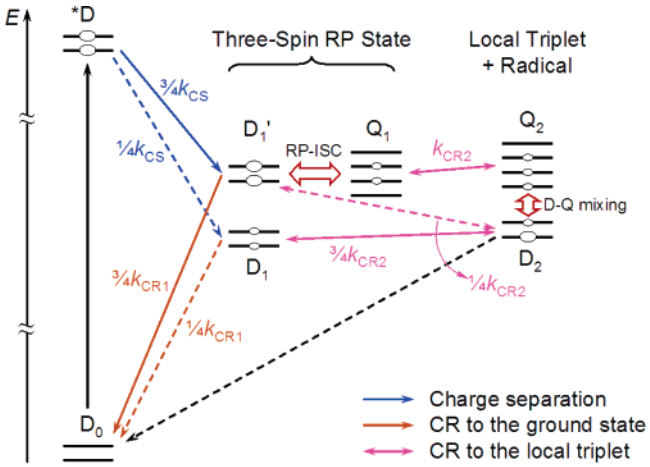

Figure 7. Energy level diagram showing the spin manifolds of **7** after charge separation and charge recombination in an external magnetic field of about 0.35 T. Blue arrows denote charge separation forming the three-spin RP state; orange arrows, charge recombination to the ground doublet state; and magenta arrows, reversible D−D and Q−Q charge recombination steps leading to the local triplet ^{3}*NI, which is nearly isoenergetic with the triradical state in toluene (see text). D_1, D_1', and Q_1 form a complete spin basis set of the triradical state. Dashed lines mean less probable transitions. Red double arrows stand for processes that mix certain Zeeman levels of the relevant D and Q states. The size of the ellipse on each spin level represents its population qualitatively.

Magnetic field effect[51] and time-resolved EPR[50] experiments have shown that the exchange coupling $2J_{12}$ between MeOAn$^{\bullet+}$ and NI$^{\bullet-}$ within the RP state of model compound **8** is 1.5 ± 0.3 mT. MFE data presented in Figure 4 show that photogeneration of this same pair of radicals in **7** also yields $2J_{12}$ = 1.5 ± 0.3 mT. Finally, the exchange coupling $2J_{13}$ between MeOAn$^{\bullet+}$ and NN• should also be ~1 mT due to the similar spin−spin distances and bonding framework linking MeOAn$^{\bullet+}$ and NN• compared to those for MeOAn$^{\bullet+}$ and NI$^{\bullet-}$.

These noncommutative exchange interactions remix the spin manifold into two doublet states and a quartet state,[32] shown in Figure 7 as D_1, D_1', and Q_1 states. The energy splitting between the D_1 and D_1' (Q_1) states is large due to the magnitude of $2J_{23}$, while the splittings between the sublevels within D_1' and Q_1 are small due to the values of $2J_{12}$ and $2J_{13}$. Thus, the well-known S−T_0 mixing mechanism[51,86,98,99] of RP-ISC directly translates into $D'_{\pm1/2}$−$Q_{\pm1/2}$ mixing in this context, and TREPR spectra with the same polarization pattern should be observed. This is a consequence of the fact that the Zeeman splitting between the two spin sublevels of D_1', namely ~0.35 T or ~10^{-5} eV, is negligible compared to the overall free energy change for charge separation, ΔG(*D → D_1') = −0.8 eV (see Figure 2), producing an unpolarized D_1' state (ignoring thermal polarization), which is analogous to the singlet RP produced in model systems such as **8** (Figure 7). The Q_1 state is not populated initially as a result of spin conservation. The D_1 state, which is energetically far removed from the D_1' and Q_1 states, does not mix with these states.

The above reasoning is justified by TREPR and MFE results for **7**, which probe the D_1'−Q_1 splitting, Δ_{DQ}, of the triradical state.[41] The experimental TREPR spectrum is simulated with a two-state-mixing model similar to the one used for reference

(90) Eaton, S. S.; Eaton, G. R. *Biol. Magn. Reson.* **2000**, *19*, 29−154.
(91) Marcus, R. A. *J. Chem. Phys.* **1965**, *43*, 679−701.
(92) Weiss, E. A.; Tauber, M. J.; Ratner, M. A.; Wasielewski, M. R. *J. Am. Chem. Soc.* **2005**, *127*, 6052−6061.
(93) Kobori, Y.; Kawai, A.; Obi, K. *J. Phys. Chem.* **1994**, *98*, 6425−6429.
(94) Mori, Y.; Sakaguchi, Y.; Hayashi, H. *J. Phys. Chem. A* **2000**, *104*, 4896−4905.
(95) Magin, I. M.; Shevel'kov, V. S.; Obynochny, A. A.; Kruppa, A. I.; Leshina, T. V. *Chem. Phys. Lett.* **2002**, *357*, 351−357.
(96) Hasharoni, K.; Levanon, H.; Greenfield, S. R.; Gosztola, D. J.; Svec, W. A.; Wasielewski, M. R. *J. Am. Chem. Soc.* **1995**, *117*, 8055−8056.
(97) Holl, N.; Port, H.; Wolf, H. C.; Strobel, H.; Effenberger, F. *J. Chem. Phys.* **1993**, *176*, 215−220.
(98) Hasharoni, K.; Levanon, H.; Greenfield, S. R.; Gosztola, D. J.; Svec, W. A.; Wasielewski, M. R. *J. Am. Chem. Soc.* **1996**, *118*, 10228−10235.
(99) Closs, G. L.; Forbes, M. D. E.; Norris, J. R. *J. Phys. Chem.* **1987**, *91*, 3592−3599.

compound **8**,[52] yielding $\Delta_{DQ} = 1.3$ mT (Figure 5A). Also, the sign of this splitting is confirmed to be positive, i.e., D_1' is higher in energy than Q_1, from the *e a* polarization pattern of the RP spectrum, using the RP sign rule[52,98] for field-swept spectra:

$$\Gamma = \mu \, \mathrm{sign}(\Delta_{DQ}) = \begin{cases} - & e\,a \\ + & a\,e \end{cases} \qquad (1)$$

where μ equals -1 or $+1$ for a doublet or a quartet precursor, the former being the case. The magnitude of the $D_1'-Q_1$ splitting, $|\Delta_{DQ}| = 1.5$ mT $\pm$ 0.3 mT, is also obtained directly from the maximum in the MFE plot shown in Figure 4, and is in good agreement with the TREPR results. Since $|\Delta_{DQ}|$ for **7** and $2J$ for the photogenerated RP state in reference molecule **8** are the same within experimental error, the presence of the third spin on NN• in the photogenerated triradical in **7** has essentially no influence on the spin−spin exchange interaction $2J_{12}$ between the two photogenerated radical ions.

Charge Recombination and Switching of the Spin Basis Set. Based on previous studies of **8**[51] and other closely related molecules,[41,75,100,101] RP-ISC in **7** is followed by charge recombination, returning part of the population to the ground state D_0 and the remainder to a state having a local triplet configuration on NI, ^{2,4}(MeOAn−6ANI−Ph(NN•)−^{3}*NI), which is nearly isoenergetic with ^{2,4}(MeOAn$^{+\bullet}$−6ANI−Ph(NN•)−NI$^{-\bullet}$) in toluene. The neutral stable radical NN• is spin coupled to NI$^{-\bullet}$ with $2J_{23} \approx 10^{-4}$ eV, and therefore it does not redirect the charge recombination but establishes a new basis set of doublet and quartet states, labeled in Figure 7 as D_2 and Q_2. Again, no spin flip is considered during charge recombination, and hence the Q_2 state inherits the population of the $\pm^1/_2$ sublevels of Q_1 generated by RP-ISC from D_1'. However, the D_2 state becomes a mixture of the D_1' and D_1 states, as pointed out by Hoytink,[102] because charge recombination is accompanied by the rise of an extremely large $2J_{22}$, the local exchange interaction between the two unpaired spins of ^{3}*NI, which is estimated to be 0.9 eV, the S_1-T_1 energy gap of NI.[100] In other words, D_0, D_2, and Q_2 form a complete basis set for the recombinant states, different from the other set, D_1, D_1', and Q_1, which characterizes the triradical state.

Consequently, charge recombination from the RP state requires switching or projection of the spin basis set. Typically, charge recombination rates depend critically on the electronic coupling matrix element *V*, including its spin component:

$$k_{CR} = (2\pi/\hbar)|V|^2(\mathrm{FCWD}) \qquad (2)$$

where FCWD is the Franck−Condon weighted density of states.[103] Upon photoexcitation, model compound **8**, which does not have NN•, forms a two-spin RP with one singlet sublevel ^{1}(MeOAn$^{+\bullet}$−6ANI−Ph−NI$^{-\bullet}$) and three triplet sublevels ^{3}(MeOAn$^{+\bullet}$−6ANI−Ph−NI$^{-\bullet}$), which subsequently recombine respectively to the ground-state singlet MeOAn−6ANI−Ph−NI and the lowest triplet state MeOAn−6ANI−Ph−^{3}*NI with rates k_{CR1} and k_{CR2}, respectively. Both recombination processes conserve the spin wave function to the zeroth order. The presence of the third spin on NN•, although it reshapes the spin wave function, has negligible effects on orbital coupling and the FCWD. Using the following spin-projection relationships (see Supporting Information),

$$\langle D_0|D_1'\rangle^2 = \langle D_2|D_1\rangle^2 = 3/4 \qquad (3a)$$

$$\langle D_2|D_1'\rangle^2 = \langle D_0|D_1\rangle^2 = 1/4 \qquad (3b)$$

$$\langle Q_2|Q_1\rangle^2 = 1 \qquad (3c)$$

the charge recombination rates from the three-spin state of **7** are related to k_{CR1} and k_{CR2} as shown in Figure 7. Note that eq 3c implies that the rate of charge recombination from the quartet triradical state Q_1 is the same as if the third spin does not exist: $k_{CR}(Q_1 \rightarrow Q_2) = k_{CR2}$. In contrast, the total observed k_{CR} from the D_1' state turns into a weighted average of k_{CR1} and k_{CR2}:

$$k_{CR}(D_1' \rightarrow D_0 + D_2) = 3/4\, k_{CR1} + 1/4\, k_{CR2} \qquad (4)$$

compared to k_{CR1} for model compound **8**. This recombination rate is similar for the D_1 state and also qualitatively correct if an effective overall decay rate out of both D_1 and D_1' states is considered. Accordingly, overall charge recombination from the triradical state is accelerated if $k_{CR2} > k_{CR1}$ and otherwise slowed. For **7**, where ^{2,4}(MeOAn$^{+\bullet}$−6ANI−Ph(NN•)−NI$^{-\bullet}$) is in equilibrium with ^{2,4}(MeOAn−6ANI−Ph(NN•)−^{3}*NI), it has been shown for closely related molecules that the net k_{CR2} is slower than k_{CR1},[92,104] and thus the lifetime of the photogenerated RP observed for **7** is extended by coupling to the third spin (101 vs 73 ns), as determined here using both nanosecond transient absorption and TREPR.

Dynamic Spin Polarization after Charge Recombination. Based on the above analysis, the observed polarization of NN• following charge recombination is unexpected (Figures 5B and 7), since all the charge separation and recombination steps as well as the RP-ISC process itself in this system do not generate a net *overall* spin polarization. The theory of chemically induced dynamic electron polarization[105] (CIDEP) has been well established for doublet−doublet[86,99,106] and triplet−doublet[107−110] interactions, when these paramagnetic species diffuse in solution. Generally, overall net spin polarization can be traced back to nonadiabatic spin evolution, triggered by hyperfine interactions, spin−orbit coupling, and/or zero-field splitting (ZFS). Gast and Hoff[111,112] observed that reduction of the ubiquinone electron acceptor (UQ) in the primary electron transport cofactor sequence of bacterial photosynthetic reaction center proteins, $(BChl)_2$−BPheo−UQ$^{-\bullet}$, followed by photogeneration of the primary radical pair, $(BChl)_2^{+\bullet}$−BPheo$^{-\bullet}$−UQ$^{-\bullet}$, results in a net emissively polarized UQ$^{-\bullet}$, which they attributed to polarization transfer from the nearby BPheo$^{-\bullet}$ due to spin−

(100) Wiederrecht, G. P.; Svec, W. A.; Wasielewski, M. R.; Galili, T.; Levanon, H. *J. Am. Chem. Soc.* **2000**, *122*, 9715−9722.
(101) Greenfield, S. R.; Svec, W. A.; Wasielewski, M. R.; Hasharoni, K.; Levanon, H. *The Reaction Center of Photosynthetic Bacteria*; Michel-Beyerle, M.-E., Ed.; Springer: Berlin, 1996; pp 81−87.
(102) Hoytink, G. J. *Acc. Chem. Res.* **1969**, *2*, 114−120.
(103) Jortner, J. *J. Chem. Phys.* **1976**, *64*, 4860−4867.
(104) Weiss, E. A.; Sinks, L. E.; Lukas, A. S.; Chernick, E. T.; Ratner, M. A.; Wasielewski, M. R. *J. Phys. Chem. B* **2004**, *108*, 10309−10316.
(105) Muus, L. T.; Atkins, P. W.; McLauchlan, K. A.; Pedersen, J. B. *Chemically Induced Magnetic Polarization*; Reidel: Dordrecht; Boston, 1977.
(106) Norris, J. R.; Morris, A. L.; Thurnauer, M. C.; Tang, J. *J. Chem. Phys.* **1990**, *92*, 4239−4249.
(107) Blattler, C.; Jent, F.; Paul, H. *Chem. Phys. Lett.* **1990**, *166*, 375−380.
(108) Kawai, A.; Okutsu, T.; Obi, K. *J. Phys. Chem.* **1991**, *95*, 9130−9134.
(109) Goudsmit, G. H.; Paul, H.; Shushin, A. I. *J. Phys. Chem.* **1993**, *97*, 13243−13249.
(110) Blank, A.; Levanon, H. *J. Phys. Chem. A* **2001**, *105*, 4799−4807.
(111) Gast, P.; Hoff, A. J. *Biochim. Biophys. Acta, Bioenergetics* **1979**, *548*, 520−535.
(112) Hoff, A. J.; Gast, P. *J. Phys. Chem.* **1979**, *83*, 3355−3358.

spin exchange coupling of $BPheo^{-\bullet}$ with $UQ^{-\bullet}$. In addition, Yamauchi[85] has put forward a relaxation mechanism to account for a two-phase polarization pattern where the sign of the overall polarization switches from *a* to *e* or from *e* to *a* as time elapses, but in this case a single rise and decay with no switching of the sign of the transient polarization is observed. The experimental observation that generation of dynamic spin polarization on $NN^{\bullet}$ is synchronous with the decay of the charge-separated state suggests that the recombinant local triplet ^{3}*NI is the key to the generation of net polarization. This can be explained by the fact that the Hamiltonian that describes the ZFS of triplet states, contains the double-quantum terms S_+^2 and S_-^2 if the triplet

$$H_{ZFS} = D(S_z^2 - {}^1/_3S^2) + E(S_x^2 - S_y^2) = D(S_z^2 - {}^1/_3S^2) + {}^1/_2E(S_+^2 + S_-^2) \quad (5)$$

state is localized and E is significant. These two terms couple the $|D_2 +1/2\rangle$ sublevel, populated from the D_1 and D_1' states, and the vacant $|Q_2 -3/2\rangle$ sublevel due to their proximity in energy.[108,109,113] Consequently, a net absorptive polarization suggests that the energy level of Q_2 lies above D_2, corresponding to antiferromagnetic coupling between ^{3}*NI and $NN^{\bullet}$, so that $|D_2 +1/2\rangle$ gets depopulated by the S_-^2 term before the ground D_0 state inherits this spin polarization from D_2 and remains polarized until spin−lattice relaxation ensues.

Conclusion

We have demonstrated that the $NN^{\bullet}$ radical within a D−B($NN^{\bullet}$)−A system having well-defined distances between each component influences the spin dynamics of the photogenerated triradical states $^{2,4}[D^{+\bullet}-B(NN^{\bullet})-A^{-\bullet}]$, resulting in slower charge recombination. The observed spin−spin exchange interaction between the photogenerated radicals $D^{+\bullet}$ and $A^{-\bullet}$ is not altered by the presence of the third spin, which only accelerates radical pair intersystem crossing. Normally, the spin dynamics of correlated radical pairs do not produce a net spin polarization; however, net spin polarization appears on $NN^{\bullet}$ with the same time constant as describes the photogenerated radical ion pair decay. This effect is attributed to antiferromagnetic coupling between $NN^{\bullet}$ and the local triplet state ^{3}*NI, which is populated following charge recombination. This requires an effective switch in the spin basis set between the triradical and the three-spin charge recombination product having both $NN^{\bullet}$ and ^{3}*NI present. It remains to be seen what effect a radical having significant spin density delocalized onto the bridge has on electron transfer. If the bridge within the D−B−A system is itself a free radical, it is possible that enhanced charge and spin transport over long distances — important for both molecular electronics and photochemical energy conversion — may result. Current studies are underway to develop a D−B−A system that tests this limit.

Acknowledgment. The work was supported by the National Science Foundation under grant no. CHE-0415730 and by the Defense Advanced Research Projects Agency. E.T.C. thanks the Natural Sciences and Engineering Research Council of Canada (NSERC). E.A.W. thanks the Presidential Fellowship Program at Northwestern University for support of this work. The Bruker E580 spectrometer was purchased with partial support from NSF Grant No. CHE-0131048.

Supporting Information Available: Synthesis, ^{1}H NMR, EPR, and characterization details for all new compounds. This material is available free of charge via the Internet at http://pubs.acs.org.

JA0576435

(113) Kobori, Y.; Takeda, K.; Tsuji, K.; Kawai, A.; Obi, K. *J. Phys. Chem. A* **1998**, *102*, 5160−5170.